Streptococcus agalactiae npx Is Required for Survival in Human Placental Macrophages and Full Virulence in a Model of Ascending Vaginal Infection during Pregnancy

Jacky Lu,[a] Rebecca E. Moore,[b,c] Sabrina K. Spicer,[b] Ryan S. Doster,[c,d] Miriam A. Guevara,[a] Jamisha D. Francis,[a] Kristen N. Noble,[e] Lisa M. Rogers,[f] Julie A. Talbert,[b] ⓘ Michelle L. Korir,[g,h] ⓘ Steven D. Townsend,[b] David M. Aronoff,[f] ⓘ Shannon D. Manning,[g] ⓘ Jennifer A. Gaddy[a,c,i,j]

aDepartment of Pathology, Microbiology and Immunology, Vanderbilt University Medical Center, Nashville, Tennessee, USA
bDepartment of Chemistry, Vanderbilt University, Nashville, Tennessee, USA
cDepartment of Medicine, Vanderbilt University Medical Center, Nashville, Tennessee, USA
dDepartment of Medicine, University of Louisville, Louisville, Kentucky, USA
eDepartment of Pediatrics, Vanderbilt University Medical Center, Nashville, Tennessee, USA
fDepartment of Medicine, Indiana University, Indianapolis, Indiana, USA
gDepartment of Microbiology and Molecular Genetics, Michigan State University, East Lansing, Michigan, USA
hDepartment of Biology, Aurora University, Aurora, Illinois, USA
iTennessee Valley Healthcare Systems, Department of Veterans Affairs, Nashville, Tennessee, USA
jCenter for Medicine Health and Society, Vanderbilt University, Nashville, Tennessee, USA

ABSTRACT *Streptococcus agalactiae*, also known as group B *Streptococcus* (GBS), is a Gram-positive encapsulated bacterium that colonizes the gastrointestinal tract of 30 to 50% of humans. GBS causes invasive infection during pregnancy that can lead to chorioamnionitis, funisitis, preterm prelabor rupture of membranes (PPROM), preterm birth, neonatal sepsis, and maternal and fetal demise. Upon infecting the host, GBS encounters sentinel innate immune cells, such as macrophages, within reproductive tissues. Once phagocytosed by macrophages, GBS upregulates the expression of the gene *npx*, which encodes an NADH peroxidase. GBS mutants with an *npx* deletion (Δ*npx*) are exquisitely sensitive to reactive oxygen stress. Furthermore, we have shown that *npx* is required for GBS survival in both THP-1 and placental macrophages. In an *in vivo* murine model of ascending GBS vaginal infection during pregnancy, *npx* is required for invading reproductive tissues and is critical for inducing disease progression, including PPROM and preterm birth. Reproductive tissue cytokine production was also significantly diminished in Δ*npx* mutant-infected animals compared to that in animals infected with wild-type (WT) GBS. Complementation in *trans* reversed this phenotype, indicating that *npx* is critical for GBS survival and the initiation of proinflammatory signaling in the gravid host.

IMPORTANCE This study sheds new light on the way that group B *Streptococcus* (GBS) defends itself against oxidative stress in the infected host. The enzyme encoded by the GBS gene *npx* is an NADH peroxidase that, our study reveals, provides defense against macrophage-derived reactive oxygen stress and facilitates infections of the uterus during pregnancy. This enzyme could represent a tractable target for future treatment strategies against invasive GBS infections.

KEYWORDS *Streptococcus*, infection, innate immunity, reactive oxygen species, ROS

Preterm deliveries occur at less than 37 weeks of gestation (1). Despite advancing knowledge of risk factors and the introduction of public health and medical interventions to reduce the occurrence, the rate of preterm birth (PTB) in the United States

and other developed countries still hovers at between 5 and 9% (2, 3). Preterm births account for 75% of perinatal mortality and over 50% of long-term morbidity (4). While most preterm babies survive, these infants are at an increased risk of neurodevelopmental impairments, respiratory conditions, and gastrointestinal complications (5). Intrauterine infection may account for at least 25 to 40% of preterm births (6).

Streptococcus agalactiae, or group B *Streptococcus* (GBS), is an encapsulated Gram-positive bacterium that colonizes the urogenital tract and lower gastrointestinal tract of 30% of healthy adults (7). Although GBS is a common member of the intestinal microbiota, it can cause invasive infections during pregnancy, leading to sepsis or meningitis in the neonate (8). Indeed, GBS is a leading cause of adverse pregnancy and neonatal outcomes such as stillbirth, chorioamnionitis, preterm birth, and neonatal sepsis (9); up to 25% of invasive GBS infections during pregnancy end in stillbirth or spontaneous abortion (10). To prevent neonatal infection, the Centers for Disease Control and Prevention (CDC) recommends screening mothers for GBS late in the third trimester and administering antibiotic therapy to those who test positive during labor (11). There is a concern, however, that antibiotic exposure could alter the infant's developing microbiome, which may contribute to lifelong consequences (8), and intrapartum antibiotic prophylaxis does not prevent late-onset disease, stillbirth, or preterm birth (12). Consequently, GBS remains the leading infectious cause of morbidity and mortality among neonates in the United States (13).

GBS pathogenesis begins with adherence to vaginal epithelial cells (8). For successful colonization, the bacteria can form biofilm structures to evade the immune system (14). Following vaginal colonization, GBS can ascend above the cervical os, through as-yet-undefined mechanisms, and traverse the fetal membranes, causing fetal infection (15). The inflammation of extraplacental ("fetal") membranes in response to GBS infection is termed chorioamnionitis (16).

Because the human immune system has evolved to protect against pathogens, this paradigm is more complex during pregnancy as the system must defend the gravid uterus against infection and maintain immunologic tolerance to the semiallogeneic fetus. This careful balance must be maintained to prevent harm to the mother and fetus. Consequently, the immune response during pregnancy is characterized by dynamic modifications of the maternal and fetal tissues reliant on the stage of pregnancy (17, 18). Bacteria commonly cause intrauterine infections, triggering a proinflammatory response originating in the decidua by the activation of pattern recognition receptors (PRRs), which may result in preterm birth (19, 20). Previous mouse studies have demonstrated that innate immune signaling is sufficient to instigate adverse pregnancy outcomes (18). The presence of proinflammatory cytokines, including interleukin-1β (IL-1β), IL-6, IL-8, and tumor necrosis factor alpha (TNF-α), in the amnionic fluid or cervicovaginal lavage fluid of patients is indicative of the onset of preterm labor (21–23). A variety of leukocytes responsible for cytokine production are present in the reproductive tissues, including maternal natural killer cells, dendritic cells, macrophages, and lymphocytes (24). In particular, macrophages represent a predominant subset of human leukocytes that serve as antigen-presenting cells (APCs) in the decidua, comprising 20 to 25% of all decidual leukocytes (25).

Placental macrophages (PMs) represent a mixed population of maternally and fetally derived cells (26) that are thought to play critical roles in placental invasion, angiogenesis, tissue modeling, and development (27, 28). Recently, studies have demonstrated that PMs defend against invading bacterial pathogens by the release of macrophage extracellular traps (29).

Upon phagocytosis by a macrophage, bacterial pathogens are trapped in a phagosome, which is a highly oxidative environment (30). Additionally, cells generate reactive oxygen species (ROS) as metabolic by-products. The level of ROS produced by the NOX2 NADPH oxidase in macrophages is significantly higher under conditions of infection than in resting states; hence, stimulating oxidative stress to kill invading pathogens is a critical pathway for innate immunity (30). ROS can damage macromolecules, including lipids, proteins, and nucleic acids, ultimately leading to cell death (31). Bacterial pathogens have evolved strategies to survive in highly oxidative environments, such as by producing antioxidants or enzymes that can inactivate and detoxify ROS (32). GBS produces several products to help circumnavigate ROS stress during infection, including superoxide dismutase, which
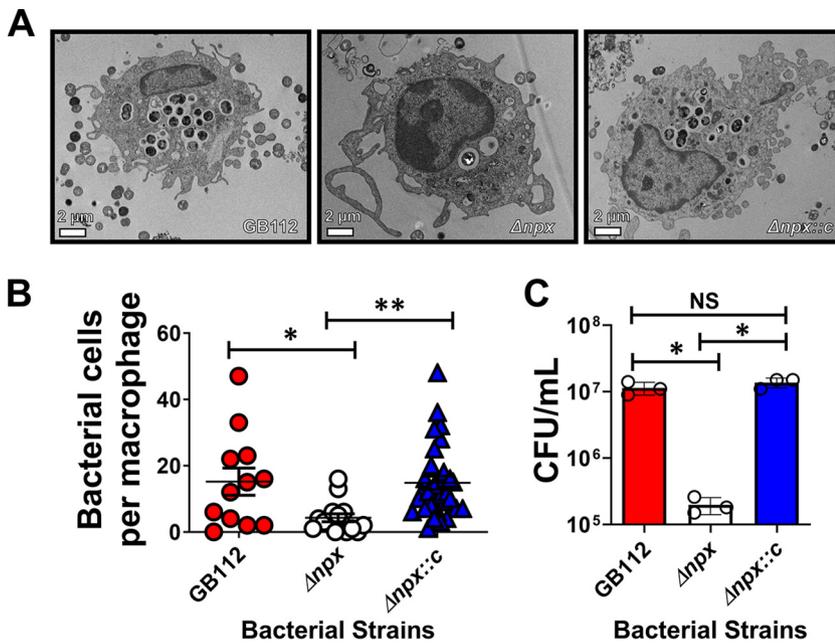
FIG 1 Analysis of GBS survival in primary human placental macrophage cells. (A) Transmission electron microscopy analyses reveal that *npx* is required for GBS survival in placental macrophages. (B) Enumeration of bacterial cells per placental macrophage via electron microscopy analyses indicates that WT GBS (GB112) (red) survives within primary human placental macrophages, but an isogenic Δ*npx* mutant (white) is attenuated in intracellular survival compared to both the parental strain (GB112) and the complemented derivative (Δ*npx::c*) (blue). (C) Quantitative culture analysis of bacterial survival by gentamicin protection assays reveals that *npx* is required for GBS survival in placental macrophages. *, $P < 0.05$; **, $P < 0.01$ (by one-way ANOVA with Tukey's *post hoc* multiple-comparison test). NS, statistically indistinguishable (3 biological replicates).

converts superoxide to H_2O_2 and O_2 (33). GBS also produces glutathione and a carotenoid pigment, which protect against oxidative damage (34, 35). A previous study revealed that GBS *npx* encodes an NADH peroxidase that is critical for the detoxification of and resistance to peroxide stress and survival within THP-1 macrophage-like cells (36). The deletion of the *npx* locus in a Δ*npx* mutant resulted in an attenuated ability to detoxify peroxide, a result that was reversed via genetic complementation in *trans* (36).

During ascending vaginal infections in pregnancy, some of the first immune cells that GBS encounters at the maternal-fetal interface are placental macrophages. We hypothesized that *npx* is also required for GBS to survive within PMs and to cause disease progression during pregnancy. To test this, we sought to characterize its role in pathogenesis *in vivo* using an established pregnant mouse model of ascending vaginal infection and *ex vivo* using primary human PMs. Here, we demonstrate that *npx* is required for GBS survival in PMs, full virulence, and invasion of gravid reproductive tissues *in vivo*. We have also demonstrated that *npx* is required for the induction of specific inflammatory cytokines expressed during GBS infection.

RESULTS

Transmission electron microscopy visualization of intracellular GBS in placental macrophages. Transmission electron microscopy (TEM) was used to visualize intracellular GB112 and isogenic mutants in PMs. This analysis revealed that few intracellular Δ*npx* cells were observed compared to wild-type (WT) GB112 and an isogenic complemented Δ*npx* derivative harboring a plasmid containing the *npx* locus (Δ*npx::c*) (Fig. 1A). Indeed, PM samples infected with WT GB112 averaged 17 bacterial cells per macrophage, while PMs infected with the Δ*npx* mutant averaged 5 bacterial cells per macrophage. This result was reversed in the strain with a genetic complementation of the *npx* allele in *trans*, which infected an average of 16 bacterial cells per macrophage (Fig. 1B). Quantitative culture analyses of living bacterial cells in PMs via gentamicin
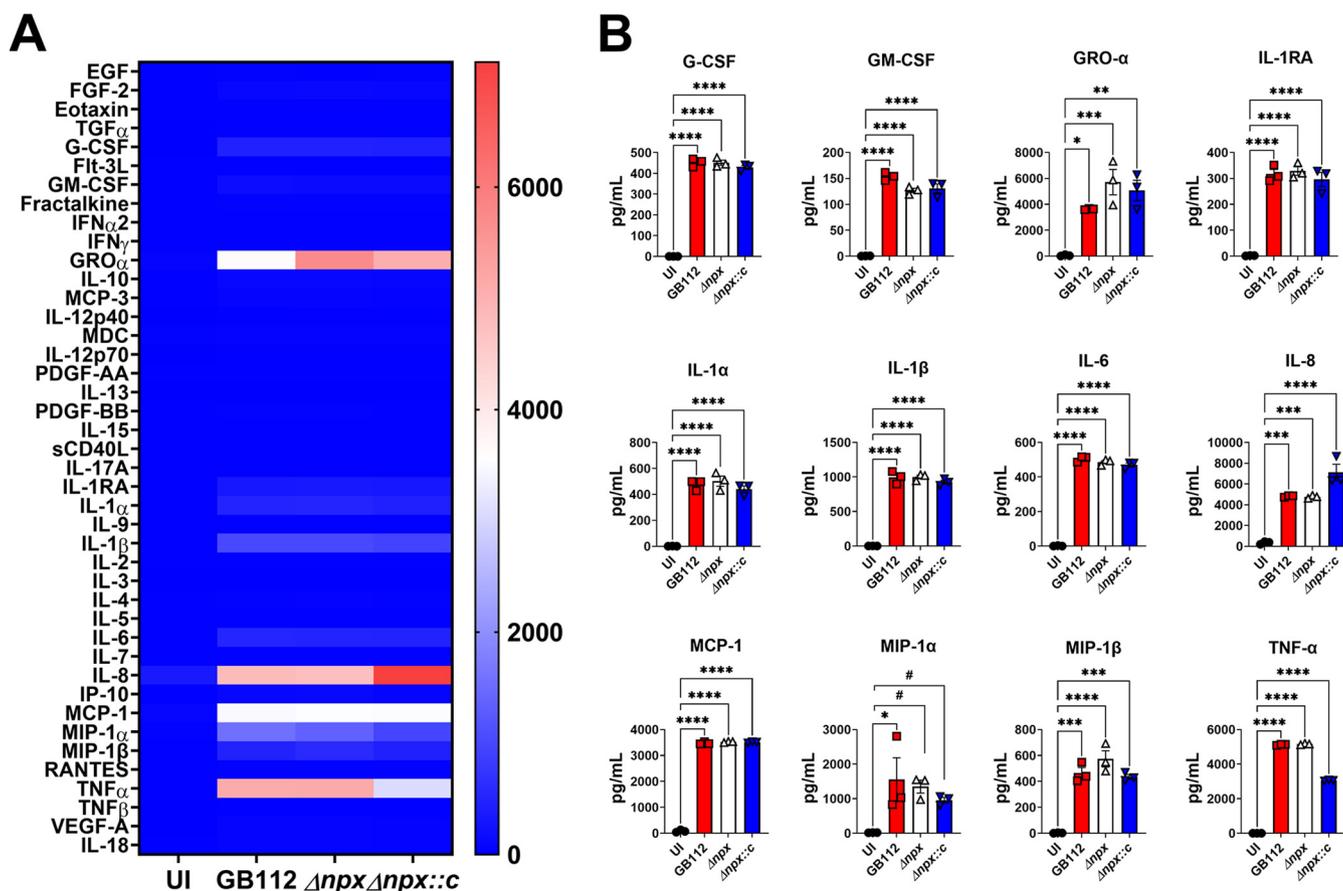
FIG 2 GBS *npx* expression is dispensable for the initiation of proinflammatory cytokine production by human placental macrophages. (A) Heat map results (blue, low levels; red, high levels) of multiplex cytokine analyses of primary human placental macrophage-secreted fractions after coculture with wild-type GB112, the isogenic Δ*npx* mutant, or the isogenic complemented Δ*npx* derivative (Δ*npx::c*) reveal that GBS infection induces the production of multiple proinflammatory cytokines compared to the uninfected controls (UI). EGF, epidermal growth factor; FGF, fibroblast growth factor; TGFα, transforming growth factor α; IFNα2, interferon alpha 2; PDGF-AA, platelet-derived growth factor AA; sCD40L, soluble CD40 ligand; VEGF-A, vascular endothelial growth factor A. (B) Quantitation of cytokine levels reveals the significantly enhanced production of G-CSF, GM-CSF, GRO-α, IL-1RA, IL-1α, IL-1β, IL-6, IL-8, MCP-1, MIP-1α, MIP-1β, and TNF-α in macrophages cocultured with the GB112 (red), Δ*npx* (white), and Δ*npx::c* (blue) strains compared to the uninfected controls (black). *, $P < 0.05$; **, $P < 0.01$; ***, $P < 0.001$; ****, $P < 0.0001$ (by one-way ANOVA with Tukey's *post hoc* multiple-comparison test). #, $P < 0.05$ (by Student's *t* test with Welch's correction) (3 biological replicates).

protection assays demonstrated that an average of 1.1×10^7 WT GBS cells survived per 5×10^5 to 1×10^6 macrophages, compared to an average of 2.0×10^5 cells for the Δ*npx* mutant ($P < 0.05$ by one-way analysis of variance [ANOVA] with Tukey's *post hoc* test) (Fig. 1C). Meanwhile, complementation with the Δ*npx::c* vector restored survival inside macrophages, with an average of 1.4×10^7 cells surviving per 5×10^5 to 1×10^6 macrophages, a result that was comparable to those for WT GB112 ($P < 0.01$ by one-way ANOVA with Tukey's *post hoc* test). Taken together, these results show that *npx* plays an important role in persistence and survival within PMs.

Placental macrophage cytokine responses to intracellular GBS infection. Because we observed a difference in intracellular survival among the GB112 (WT), Δ*npx*, and Δ*npx::c* strains, we hypothesized that there may be differences in cytokine production by PMs. Following infection of PMs with GBS and its isogenic mutants overnight, the cell supernatants were collected, and cytokine quantifications were performed. Intracellular infection with WT GB112 resulted in the increased secretion of a variety of proinflammatory cytokines, including CXC motif ligand 1 (CXCL1), interleukin 1 receptor antagonist (IL-1RA), interleukin 1α (IL-1α), interleukin 1β (IL-1β), interleukin 6 (IL-6), interleukin 8 (IL-8), monocyte chemoattractant protein 1 (MCP-1), macrophage inflammatory protein 1α (MIP-1α), macrophage inflammatory protein 1β (MIP-1β), and tumor necrosis factor alpha (TNF-α) (Fig. 2). Nonetheless, these cytokines were similarly increased in PMs infected with the Δ*npx* and
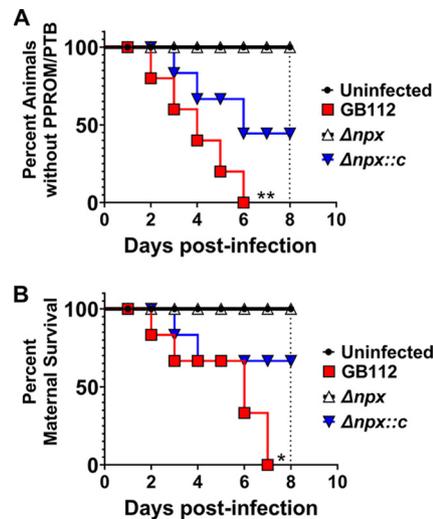
FIG 3 Analysis of the role of GBS *npx* in disease progression in a mouse model of ascending vaginal infection during pregnancy. (A) Evaluation of the incidence of (percentage of animals exhibiting) preterm premature rupture of membranes (PPROM) and preterm birth (PTB) over time (8 days postinfection and term for gestation). Wild-type GB112-infected animals (red) had higher incidences of PPROM and PTB than did uninfected (black) and Δ*npx* mutant-infected (white) animals, with 100% of the GB112-infected cohort experiencing PPROM or PTB by 6 days postinfection. Complementation of the *npx* locus in *trans* (Δ*npx::c*) (blue) resulted in 65% PTB and PPROM by 6 days postinfection. (B) Evaluation of maternal mortality over time (8 days postinfection and term for gestation). GB112-infected animals had a 100% maternal mortality rate by 7 days postinfection, a rate that was significantly higher than those for the uninfected control and Δ*npx* mutant-infected cohorts, which exhibited 0% maternal mortality by 8 days postinfection. Complementation in *trans* partially restored mortality (33% maternal death by 8 days postinfection) (n = 6 to 9 dams total from 3 separate experiments) (*, P < 0.05; **, P < 0.01 [by a Mantel-Cox log rank test and a Gehan-Breslow-Wilcoxon test]).

Δ*npx::c* strains, suggesting that *npx* does not influence the production of proinflammatory cytokines by PMs *ex vivo*.

GBS *npx* is associated with preterm birth in a mouse model of ascending infection. To assess the role of GBS *npx in vivo* in the context of ascending infection during pregnancy, we utilized a pregnant mouse model initiated by intravaginal GBS infection (37). Previous work demonstrated that in this model, ascending vaginal GBS infection results in bacterial invasion, inflammation of reproductive tissues, preterm prelabor rupture of membranes (PPROM), preterm birth (PTB), as well as maternal and neonatal demise (37). Hence, we hypothesized that Npx could be important for GBS evasion of innate immune responses in the gravid reproductive tract. Our results (Fig. 3) demonstrate that mice infected with WT GB112 had higher incidences of PPROM and PTB than did uninfected and Δ*npx* mutant-infected animals (P = 0.0024 by a Mantel-Cox log rank test and P = 0.0067 by a Gehan-Breslow-Wilcoxon test). Notably, all GB112-infected animals experienced PPROM or PTB by 6 days postinfection. Complementation of the *npx* locus in *trans* resulted in 65% PTB and PPROM by 6 days postinfection; these results were statistically indistinguishable from those for cohorts infected with WT GB112 (P = 0.0766 by a Mantel-Cox log rank test and P = 0.1135 by a Gehan-Breslow-Wilcoxon test). By 7 days postinfection, GB112-infected animals had a 100% maternal mortality rate, which was significantly higher than that for the uninfected controls and Δ*npx* mutant-infected cohorts, which exhibited 0% maternal mortality by 8 days postinfection (P = 0.0164 by a Mantel-Cox log rank test and P = 0.0442 by a Gehan-Breslow-Wilcoxon test). Complementation in *trans* partially decreased the mortality rate (33% maternal death by 8 days postinfection), which was statistically indistinguishable from that for WT GB112 (P = 0.2205 by a Mantel-Cox log rank test and P = 0.4190 by a Gehan-Breslow-Wilcoxon test).

Analysis of bacterial burdens in reproductive tissues. To quantify the bacterial burden and classify host responses within reproductive tissues, intravaginal infections were performed using an infectious dose of 5×10^2 to 1×10^3 CFU. Mice were sacrificed at 48 h postinfection to collect reproductive tissues for bacteriological and immunological
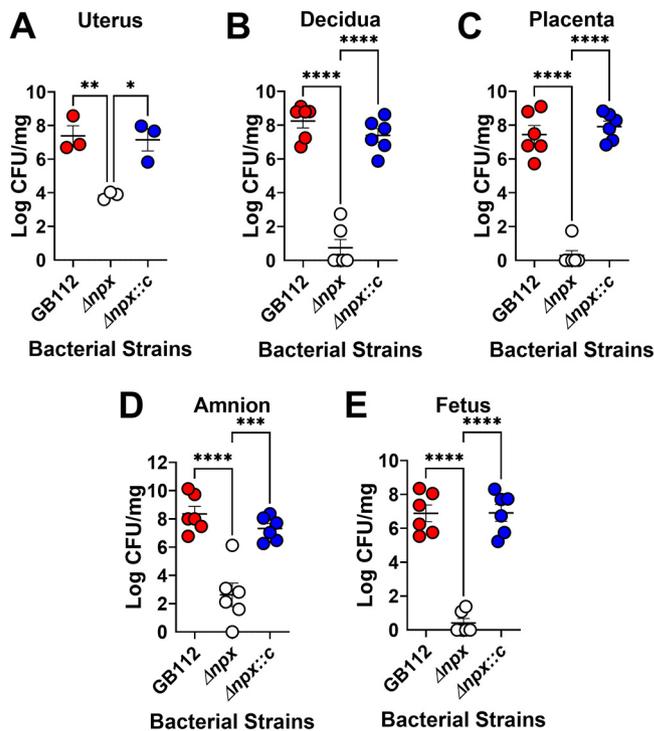
FIG 4 Analysis of bacterial burdens within gravid reproductive tissues. Shown are data from quantitative culture analyses of the bacterial burdens within the uterus (A), decidua (B), placenta (C), amnion (D), and fetus (E) of pregnant mice on embryonic day 15.5, 2 days after infection with either WT GBS (GB112) (red), an isogenic Δ*npx* mutant (white), or the isogenic complemented derivative (Δ*npx::c*) (blue). GBS *npx* is required for full bacterial burdens in reproductive tissues in a model of ascending infection during pregnancy. *, $P < 0.05$; **, $P < 0.01$; ***, $P < 0.001$; ****, $P < 0.0001$ (by one-way ANOVA with Tukey's *post hoc* multiple-comparison test) ($n = 3$ dams total, with 1 to 2 fetal-placental units analyzed per dam).

analyses. The bacterial burden was evaluated by quantitative culture methods for reproductive tissues, including uterine, decidual, placental, amnion, and fetal tissues (Fig. 4). The Δ*npx* mutant exhibited a 3.5-log decrease in the burden in uterine tissue compared to the parental strain ($P < 0.01$ by one-way ANOVA with Tukey's *post hoc* multiple-comparison test). Genetic complementation in *trans* resulted in a significant increase in the bacterial burden ($P < 0.05$ by one-way ANOVA with Tukey's *post hoc* multiple-comparison test) compared to the Δ*npx* mutant. The Δ*npx* mutant exhibited a 7.5-log decrease in the burden in decidual tissue compared to the parental strain ($P < 0.0001$ by one-way ANOVA with Tukey's *post hoc* multiple-comparison test). Genetic complementation in *trans* resulted in a significant increase in the bacterial burden ($P < 0.0001$ by one-way ANOVA with Tukey's *post hoc* multiple-comparison test) compared to the Δ*npx* mutant. The Δ*npx* mutant exhibited a 7.2-log decrease in the burden in placental tissue compared to the parental strain ($P < 0.0001$ by one-way ANOVA with Tukey's *post hoc* multiple-comparison test). Genetic complementation in *trans* resulted in a significant increase in the bacterial burden ($P < 0.0001$ by one-way ANOVA with Tukey's *post hoc* multiple-comparison test) compared to the Δ*npx* mutant. The Δ*npx* mutant exhibited a 5.7-log decrease in the burden in amnion tissue compared to the parental strain ($P < 0.0001$ by one-way ANOVA with Tukey's *post hoc* multiple-comparison test). Genetic complementation in *trans* resulted in a significant increase in the bacterial burden ($P < 0.001$ by one-way ANOVA with Tukey's *post hoc* multiple-comparison test) compared to the Δ*npx* mutant. The Δ*npx* mutant exhibited a 6.5-log decrease in the burden in fetal tissue compared to the parental strain ($P < 0.0001$ by one-way ANOVA with Tukey's *post hoc* multiple-comparison test). Genetic complementation in *trans* resulted in a significant increase in the bacterial burden ($P < 0.0001$ by one-way ANOVA with Tukey's *post hoc* multiple-comparison test) compared to the Δ*npx* mutant. This *in vivo* study revealed that Npx is required for GBS to achieve full

bacterial burdens in reproductive tissues in a model of ascending infection during pregnancy.

Analysis of bacterial growth in amniotic fluid. Because the Δ*npx* mutant exhibited attenuated bacterial burdens within reproductive tissues compared to the WT or the complemented derivative, we hypothesized that the Δ*npx* mutant might have an attenuated ability to grow in certain environments such as amniotic fluid. To test this, we utilized human and mouse amniotic fluid and performed an inoculation with WT GBS, the Δ*npx* mutant, or the complemented derivative at a 1:100 dilution. Samples were incubated overnight, and viable bacteria were enumerated via serial dilution and quantitative culture techniques. The results indicate that the Δ*npx* mutant is attenuated in its ability to grow in human amniotic fluid and mouse amniotic fluid ($P < 0.001$ and $P < 0.0001$, respectively, by one-way ANOVA with Tukey's *post hoc* multiple-comparison test), results that were reversed by genetic complementation techniques (see Fig. S1 in the supplemental material).

Expression of GBS *npx* alters cytokine responses to GBS infection. Because the Δ*npx* mutant showed decreased bacterial burdens and disease progression in the pregnant mice, we hypothesized that these could be attributed to changes in proinflammatory cytokine production as a consequence of bacterial infection. To test this, we utilized multiplex cytokine assays to quantify the repertoire of cytokines and chemokines produced within reproductive tissues in response to GBS infection and compared them to those produced in uninfected animal tissues. Our results indicate that infection with WT GBS significantly enhanced the production of IL-1β, MIP-1α, and TNF-α in the uterus, decidua, placenta, amnion, and fetus (Fig. 5 to 9 and Fig. S2 to S6) compared to the uninfected controls (*, $P < 0.05$ by one-way ANOVA; #, $P < 0.05$ by Student's *t* test). Importantly, the deletion of the *npx* gene resulted in the significantly reduced production of these cytokines and chemokines compared to the levels in WT-infected samples (*, $P < 0.05$ by one-way ANOVA; #, $P < 0.05$ by Student's *t* test). Similarly, granulocyte colony-stimulating factor (G-CSF), MCP-1, MIG, and MIP-2 were significantly upregulated in the uterus, decidua, placenta, and amnion of animals infected with WT GBS compared to the uninfected animals (*, $P < 0.05$ by one-way ANOVA; #, $P < 0.05$ by Student's *t* test), and the loss of the *npx* gene resulted in significant reductions in the production of these cytokines and chemokines compared to the levels in WT-infected samples (*, $P < 0.05$ by one-way ANOVA; #, $P < 0.05$ by Student's *t* test). IL-6 and MIP-1 were upregulated in the uterus, decidua, placenta, and fetus in response to WT GBS infection compared to the uninfected controls, and the deletion of the *npx* gene revealed significant reductions in the production of these cytokines and chemokines compared to the levels in WT-infected samples (*, $P < 0.05$ by one-way ANOVA; #, $P < 0.05$ by Student's *t* test). IP-10 was upregulated in the uterus, decidua, and placenta in response to WT GBS infection compared to the uninfected controls, and significant reductions in the production of these cytokines and chemokines were observed with the inactivation of the *npx* gene compared to the levels in WT-infected samples (*, $P < 0.05$ by one-way ANOVA; #, $P < 0.05$ by Student's *t* test). Complementation with the WT *npx* allele in *trans* restored cytokine and chemokine production to levels that were similar to those observed in WT GBS-infected animals or significantly higher than those measured in the isogenic Δ*npx* mutant-infected samples (*, $P < 0.05$ by one-way ANOVA; #, $P < 0.05$ by Student's *t* test; NS, not statistically significant [statistically indistinguishable from WT GBS]).

Infection with WT GBS resulted in the significantly enhanced production of select cytokines and chemokines, including eotaxin, G-CSF, granulocyte-macrophage colony-stimulating factor (GM-CSF), IL-1α, IL-1β, IL-6, IL-15, IP-10, KC, LIF, LIX, MCP-1, MIG, MIP-1α, MIP-1β, MIP-2, and TNF-α in the uterus (Fig. 5 and Fig. S2); eotaxin, granulocyte colony stimulating factor (G-CSF), granulocyte macrophage colony stimulating factor (GM-CSF), IL-1α, IL-1β, IL-6, IL-15, IP-10, KC, LIF, LIX, MCP-1, MIG, MIP-1α, MIP-1β, MIP-2, and TNF-α in the uterus (Fig. 5 and Fig. S2); eotaxin, G-CSF, GM-CSF, macrophage colony-stimulating factor (M-CSF), IL-1α, IL-1β, IL-6, interleukin 15 (IL-15), interferon gamma induced protein 10 (IP-10), keratinocyte chemoattractant (KC), leukemia
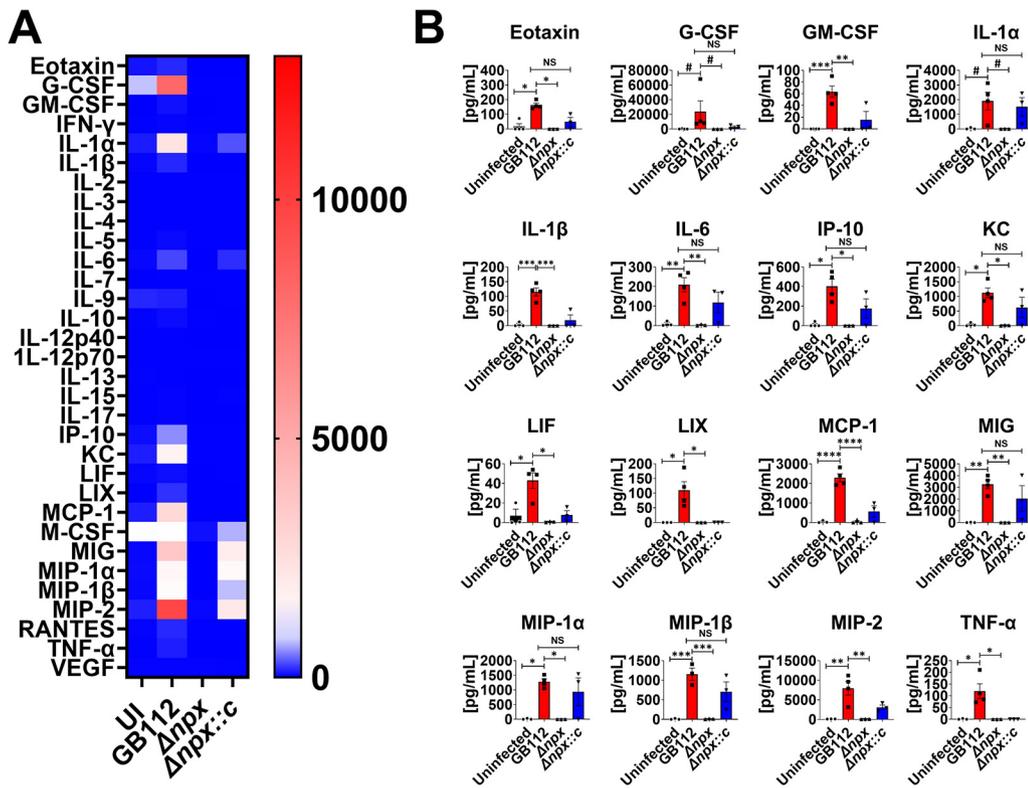
FIG 5 Analysis of cytokine production in uterus tissue in response to GBS infection. (A) Heat map results (blue, low levels; red, high levels) of multiplex cytokine analyses of gestational tissues after ascending vaginal infection with wild-type GB112, the Δnpx isogenic mutant, or the isogenic complemented Δnpx derivative (Δnpx::c) as well as the uninfected controls (UI). Uterine tissues were collected from pregnant mice on embryonic day 15.5, 2 days after vaginal infection with GBS. (B) Quantification of eotaxin, G-CSF, GM-CSF, IL-1α, IL-1β, IL-6, IP-10, KC, LIF, LIX, MCP-1, MIG, MIP-1α, MIP-1β, MIP-2, and TNF-α levels revealed that wild-type GB112 infection (red bars) significantly enhances the production of these cytokines compared to the levels in the uninfected controls (black bars), but the isogenic Δnpx mutant (white bars) is significantly attenuated in its ability to induce these cytokines compared to the parental strain. Conversely, the complemented derivative (Δnpx::c) (blue bars) is often statistically indistinguishable from the parental strain (not statistically significant [NS]). Bars indicate mean values ± standard errors of the means, with individual data points representing results from uterus tissues from individual dams. #, $P < 0.05$ (by Student's t test). *, $P < 0.05$; **, $P < 0.01$; ***, $P < 0.001$; ****, $P < 0.0001$ (by one-way ANOVA with Tukey's *post hoc* multiple-comparison test). The results indicate that GBS *npx* is required for the full initiation of proinflammatory cytokine responses in uterine tissues in a model of ascending infection during pregnancy.

inhibitory factor (LIF), lipopolysachharide-induced CXC chemokine (LIX), Monocyte chemoattractant protein-1 (MCP-1), Monokine induced by gamma (MIG), MIP-1α, MIP-1β, MIP-2, and TNF-α in the decidua (Fig. 6 and Fig. S3); G-CSF, IL-1β, IL-6, IP-10, KC, MCP-1, MIG, MIP-1α, MIP-1β, MIP-2, M-CSF, and TNF-α in the placenta (Fig. 7 and Fig. S4); G-CSF, M-CSF, IL-1β, KC, MCP-1, MIG, MIP-1α, MIP-2, and TNF-α in the amnion (Fig. 8 and Fig. S5); and eotaxin, IL-1β, IL-6, KC, MIP-1α, MIP-1β, and TNF-α in the fetus (Fig. 9 and Fig. S6), compared to the uninfected controls (*, $P < 0.05$ by one-way ANOVA; #, $P < 0.05$ by Student's t test). The inactivation of the *npx* gene, however, evoked significant reductions in the production of many of these cytokines and chemokines compared to the levels in WT-infected samples (*, $P < 0.05$ by one-way ANOVA; #, $P < 0.05$ by Student's t test).

DISCUSSION

While GBS has been identified as a perinatal pathogen since the 1930s, there are still major gaps in the knowledge of the pathophysiology of infection and disease outcomes by this bacterium. We previously observed that GBS interacts with gestational tissue macrophages and that GBS can invade the reproductive tract in a mouse model of ascending vaginal infection during pregnancy (17, 29, 38). We sought to understand
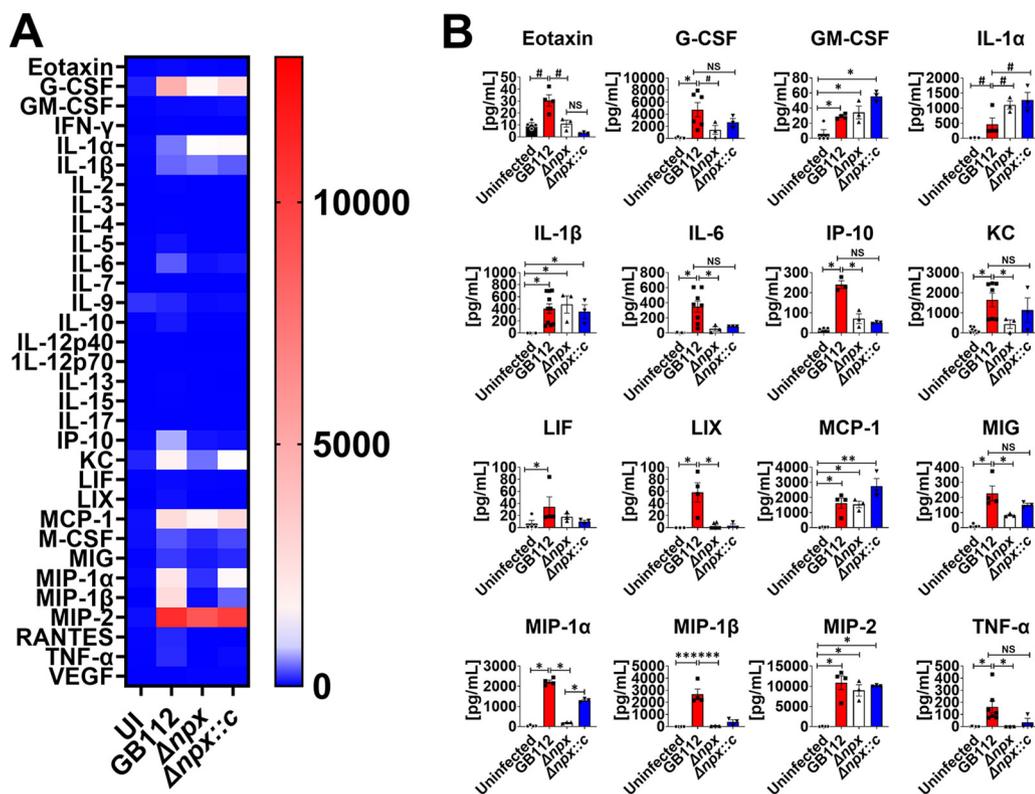
FIG 6 Analysis of cytokine production in decidua tissue in response to GBS infection. (A) Heat map results (blue, low levels; red, high levels) of multiplex cytokine analyses of decidua tissues after ascending vaginal infection with wild-type GB112, the isogenic Δ*npx* mutant (Δ*npx*), or the isogenic complemented Δ*npx* derivative (Δ*npx::c*) as well as the uninfected controls (UI). Decidua tissues were collected from pregnant mice on embryonic day 15.5, 2 days after vaginal infection with GBS. (B) Quantification of eotaxin, G-CSF, GM-CSF, IL-1α, IL-1β, IL-6, IP-10, KC, LIF, LIX, MCP-1, MIG, MIP-1α, MIP-1β, MIP-2, and TNF-α levels revealed that wild-type GB112 infection (red bars) significantly enhances the production of these cytokines compared to the levels in the uninfected controls (black bars), but the isogenic Δ*npx* mutant (white bars) is significantly attenuated in its ability to induce these cytokines compared to the parental strain. Conversely, the complemented derivative (Δ*npx::c*) (blue bars) is often statistically indistinguishable from the parental strain (not statistically significant [NS]). Bars indicate mean values ± standard errors of the means, with individual data points representing results from decidual tissues from individual fetal-placental units from separate dams. #, $P < 0.05$ (by Student's *t* test). *, $P < 0.05$; **, $P < 0.01$; ***, $P < 0.001$; ****, $P < 0.0001$ (by one-way ANOVA with Tukey's *post hoc* multiple-comparison test). The results indicate that GBS *npx* is required for the full initiation of proinflammatory cytokine responses in decidual tissues in a model of ascending infection during pregnancy.

the importance of individual GBS virulence factors that influence the outcome of GBS-macrophage interactions and might also have significance in clinical outcomes during pregnancy. We previously identified that a peroxide-detoxifying enzyme NADH peroxidase gene, *npx*, was upregulated when GBS was cultured with THP-1 macrophages (36). We further expanded that work in our current study by demonstrating that GBS *npx* aids in GBS survival within primary human placental macrophages.

Macrophages represent the second most common leukocytes within fetal membrane tissues, and these cells perform many roles, including regulating tissue remodeling during development and modulating maternal-fetal tolerance (39). Less is understood about the roles that macrophages may play during infection, as these cells are typically thought to be polarized to an anti-inflammatory M2 tolerogenic state (28). Some recent studies have noted that in response to bacteria, these cells change their polarization toward a more inflammatory M1 phenotype (40). GBS has evolved mechanisms such as a capsule to evade phagocytosis by placental macrophages (37), but once engulfed by innate immune cells, GBS deploys enhanced expression of the *npx* locus as a strategy to survive the peroxide stress encountered within the phagosomes of THP-1 macrophages (36).

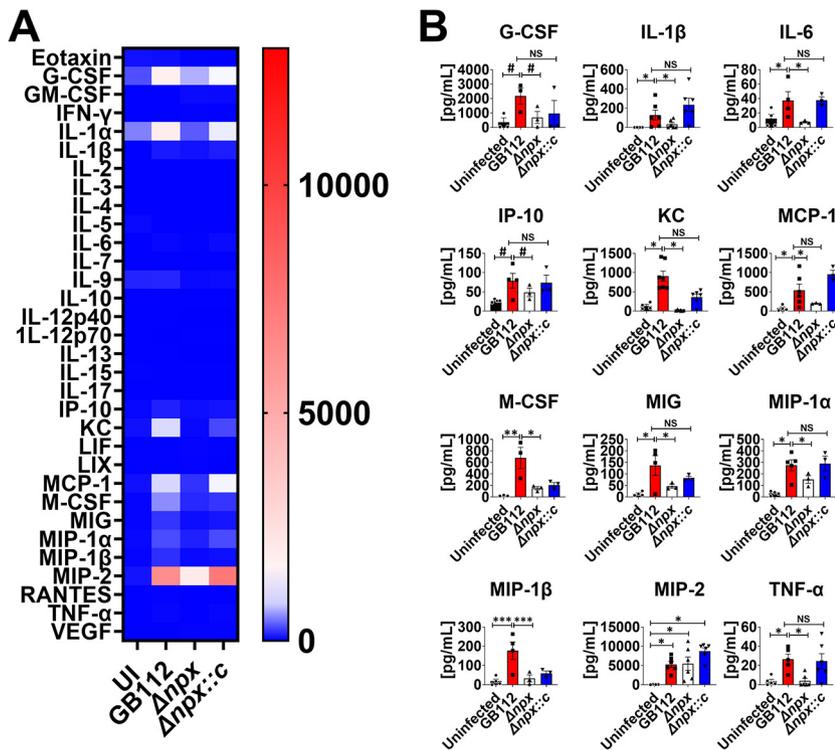Macrophages are implicated as a replicative niche for a variety of bacteria, including

FIG 7 Analysis of cytokine production in placenta tissue in response to GBS infection. (A) Heat map results (blue, low levels; red, high levels) of multiplex cytokine analyses of placenta tissues after ascending vaginal infection with wild-type GB112, the Δ*npx* isogenic mutant, or the complemented isogenic Δ*npx* derivative (Δ*npx::c*) as well as the uninfected controls (UI). Placenta tissues were collected from pregnant mice on embryonic day 15.5, 2 days after vaginal infection with GBS. (B) Quantification of G-CSF, IL-1β, IL-6, IP-10, KC, MCP-1, M-CSF, MIG, MIP-1α, MIP-1β, MIP-2, and TNF-α levels revealed that wild-type GB112 infection (red bars) significantly enhances the production of these cytokines compared to the levels in the uninfected controls (black bars), but the isogenic Δ*npx* mutant (white bars) is significantly attenuated in its ability to induce these cytokines compared to the parental strain, except for MIP-2. Conversely, the complemented derivative (Δ*npx::c*) (blue bars) is often statistically indistinguishable from the parental strain (not statistically significant [NS]). Bars indicate mean values ± standard errors of the means, with individual data points representing results from placental tissues from individual fetal-placental units from separate dams. #, $P < 0.05$ (by Student's *t* test). *, $P < 0.05$; **, $P < 0.01$; ***, $P < 0.001$; ****, $P < 0.0001$ (by one-way ANOVA with Tukey's *post hoc* multiple-comparison test). The results indicate that GBS *npx* is required for the initiation of numerous proinflammatory cytokine responses in placental tissues in a model of ascending infection during pregnancy.

Pseudomonas aeruginosa (41), *Yersinia pestis* (42), *Brucella neotomae* (43), *Escherichia coli* (44), *Neisseria gonorrhoeae* (45), and *Legionella pneumophila* (46). Recent work has demonstrated that *S. pneumoniae* can survive and replicate within splenic macrophages, which serve as a reservoir for septicemia (47), and that group A *Streptococcus* can survive and replicate within human macrophages (48). These results mirror what we observed with GBS in primary human PMs.

Furthermore, macrophages have been implicated as a potential Trojan horse aiding in the dissemination of a variety of microbial pathogens, including *Candida albicans* (49), *Mycobacterium tuberculosis* (50), *Toxoplasma gondii* (51), *Staphylococcus aureus* (52), *Cryptococcus neoformans* (53), and *Chlamydia trachomatis* (54). The depletion of host macrophages impedes *Chlamydia* and GBS dissemination in the reproductive tract (38, 55), demonstrating the important role that intracellular bacterial survival within macrophages plays in bacterial invasion of the reproductive tract. Our previous results indicate that GBS utilizes *cadD*, a metal resistance determinant, to circumnavigate metal stress within placental macrophages and to enhance bacterial ascension and invasion of the gravid reproductive tract (38). Similarly, our current work demonstrates that GBS utilizes *npx*, a peroxide resistance determinant, to circumnavigate peroxide
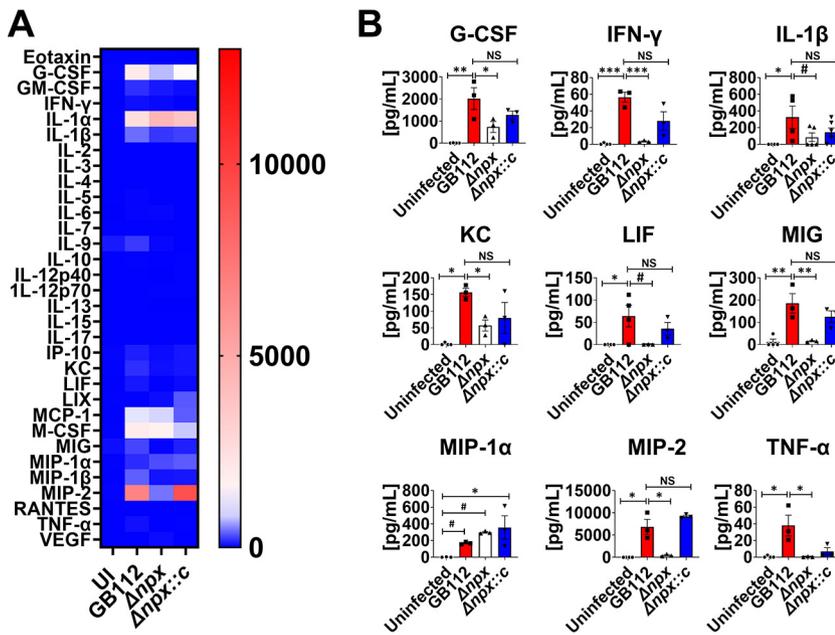
FIG 8 Analysis of cytokine production in amnion tissue in response to GBS infection. (A) Heat map results (blue, low levels; red, high levels) of multiplex cytokine analyses of amnion tissues after ascending vaginal infection with wild-type GB112, the Δ*npx* isogenic mutant, or the isogenic complemented Δ*npx* derivative (Δ*npx::c*) as well as the uninfected controls (UI). Amnion tissues were collected from pregnant mice on embryonic day 15.5, 2 days after vaginal infection with GBS. (B) Quantification of G-CSF, IFN-γ, IL-1β, KC, LIF, MIG, MIP-1α, MIP-2, and TNF-α levels revealed that wild-type GB112 infection (red bars) significantly enhances the production of these cytokines compared to the levels in the uninfected controls (black bars), but the isogenic Δ*npx* mutant (white bars) is significantly attenuated in its ability to induce these cytokines compared to the parental strain, except for MIP-1α. Conversely, the complemented derivative (Δ*npx::c*) (blue bars) is often statistically indistinguishable from the parental strain (not statistically significant [NS]). Bars indicate mean values ± standard errors of the means, with individual data points representing results from amnion tissues from individual fetal-placental units from separate dams. #, $P < 0.05$ (by Student's t test). *, $P < 0.05$; **, $P < 0.01$; ***, $P < 0.001$; ****, $P < 0.0001$ (by one-way ANOVA with Tukey's *post hoc* multiple-comparison test). The results indicate that GBS *npx* is required for the initiation of numerous proinflammatory cytokine responses in amnion tissues in a model of ascending infection during pregnancy.

stress within placental macrophages and to aid in ascending infection and disease progression during pregnancy. Taken together, these results support the hypothesis that GBS could exploit macrophages as a Trojan horse to aid in the promotion of invasive bacterial infections during pregnancy.

Upon the recognition of pathogens by immune pattern recognition receptors (PRRs) such as Toll-like receptors, a cascade of responses by the macrophage is initiated. One mechanism of defense is the phagocytosis of the bacterial cell and chemical assault within the phagosome via the deployment of peroxides and reactive oxygen species (56). Highly reactive oxygen species can damage macromolecules, including lipids, proteins, and nucleic acids, ultimately leading to cell death (30). Within the reproductive tract, invading pathogens, including *C. trachomatis* (57) and *N. gonorrhoeae* (58), are assaulted with reactive oxygen species. There is an association between *Chlamydia* and spontaneous abortion, with oxidative stress being implicated, highlighting the oxidative response in the reproductive tract against invading pathogens (57). Additionally, the presence of ROS has been demonstrated in human amniotic fluid collected in the second and third trimesters of gestation (59). This likely presents an environmental challenge for bacteria, which are highly sensitive to oxidative stress, results that are supported by the survival and growth defects observed in the Δ*npx* mutant compared to the wild type and the complemented derivative grown in human or mouse amniotic fluid.

In response to this, bacterial pathogens have evolved a range of mechanisms to
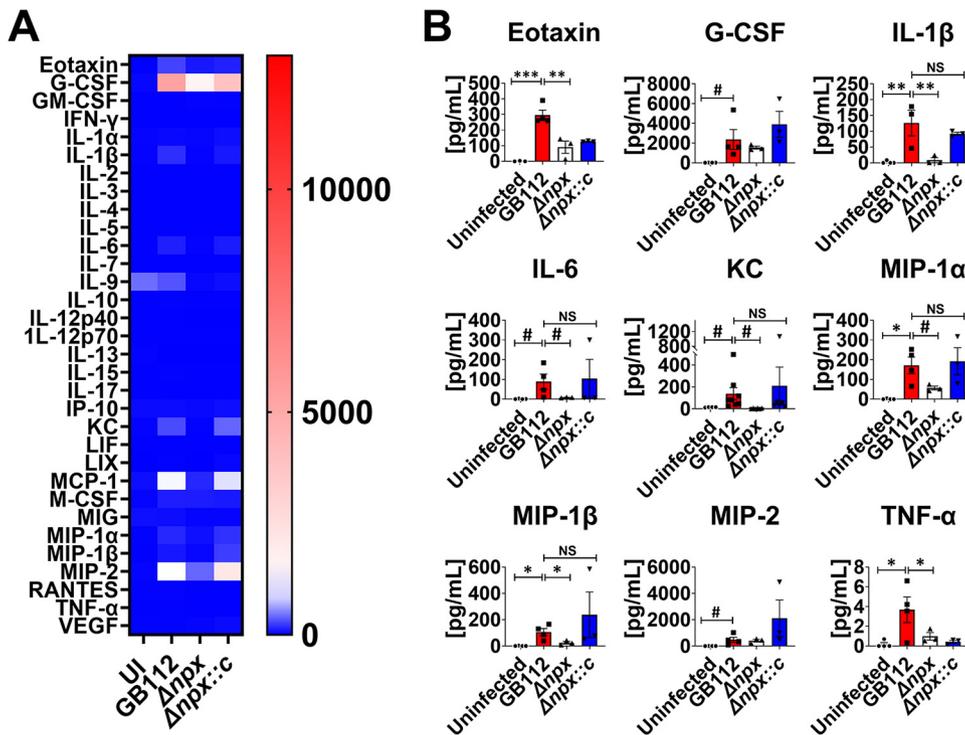
FIG 9 Analysis of cytokine production in fetus tissue in response to GBS infection. (A) Heat map results (blue, low levels; red, high levels) of multiplex cytokine analyses of fetal tissues after ascending vaginal infection with wild-type GB112, the Δ*npx* isogenic mutant, or the isogenic complemented Δ*npx* derivative (Δ*npx::c*) as well as the uninfected controls (UI). Fetus tissues were collected from pregnant mice on embryonic day 15.5, 2 days after vaginal infection with GBS. (B) Quantification of eotaxin, G-CSF, IL-1β, IL-6, KC, MIP-1α, MIP-1β, MIP-2, and TNF-α levels revealed that wild-type GB112 infection (red bars) significantly enhances the production of these cytokines compared to the levels in the uninfected controls (black bars), but the isogenic Δ*npx* mutant (white bars) is significantly attenuated in its ability to induce eotaxin, IL-1β, IL-6, KC, MIP-1α, MIP-1β, and TNF-α compared to the parental strain. Conversely, the complemented derivative (Δ*npx::c*) (blue bars) is statistically indistinguishable from the parental strain (not statistically significant [NS]) in its ability to induce IL-1β, IL-6, KC, MIP-1α, and MIP-1β. Bars indicate mean values ± standard errors of the means, with individual data points representing results from fetal tissues from individual fetuses from separate dams. #, $P < 0.05$ (by Student's *t* test). *, $P < 0.05$; **, $P < 0.01$; ***, $P < 0.001$; ****, $P < 0.0001$ (by one-way ANOVA with Tukey's *post hoc* multiple-comparison test). The results indicate that GBS *npx* is required for the initiation of numerous proinflammatory cytokine responses in fetal tissues in a model of ascending infection during pregnancy.

overcome ROS stress inside macrophages. For instance, *S. aureus* (60), *P. aeruginosa* (61, 62), *Klebsiella pneumoniae* (63), and *M. tuberculosis* (64) all express catalase to resist oxidative killing by macrophages. Other bacterial pathogens such as *E. coli* (65), *Salmonella enterica* serovar Typhi (66), and *Burkholderia pseudomallei* (67) express superoxide dismutase for the same purpose. GBS is catalase negative but expresses superoxide dismutase (SodA) (33). Our study demonstrates that the full repertoire of antioxidant defenses is required for invasive infection of the gravid reproductive tract and that the *npx*-encoded NADH peroxidase aids in GBS survival within reproductive tissue macrophages and is critical for full virulence in a pregnant animal model. Interestingly, a dye-neutralizing peroxidase (DyP) has been identified in *M. tuberculosis*, which is critical for bacterial survival within host macrophages as well (68). Similarly, in *Listeria monocytogenes*, peroxidases encoded within the *fri* and *ahpA* loci were each required for *L. monocytogenes* to survive acute peroxide stress, and the *fri* locus was essential for cytosolic growth within host macrophages (69). These studies further underscore the critical role that bacterial peroxidases play in the host-pathogen dialogue, specifically with respect to intracellular survival.

In addition to aiding in GBS intracellular survival within host immune cells, the *npx* locus is critical for virulence *in vivo*. In our mouse model of ascending vaginal infection during pregnancy, we observed that mutants lacking *npx* showed impaired invasion of
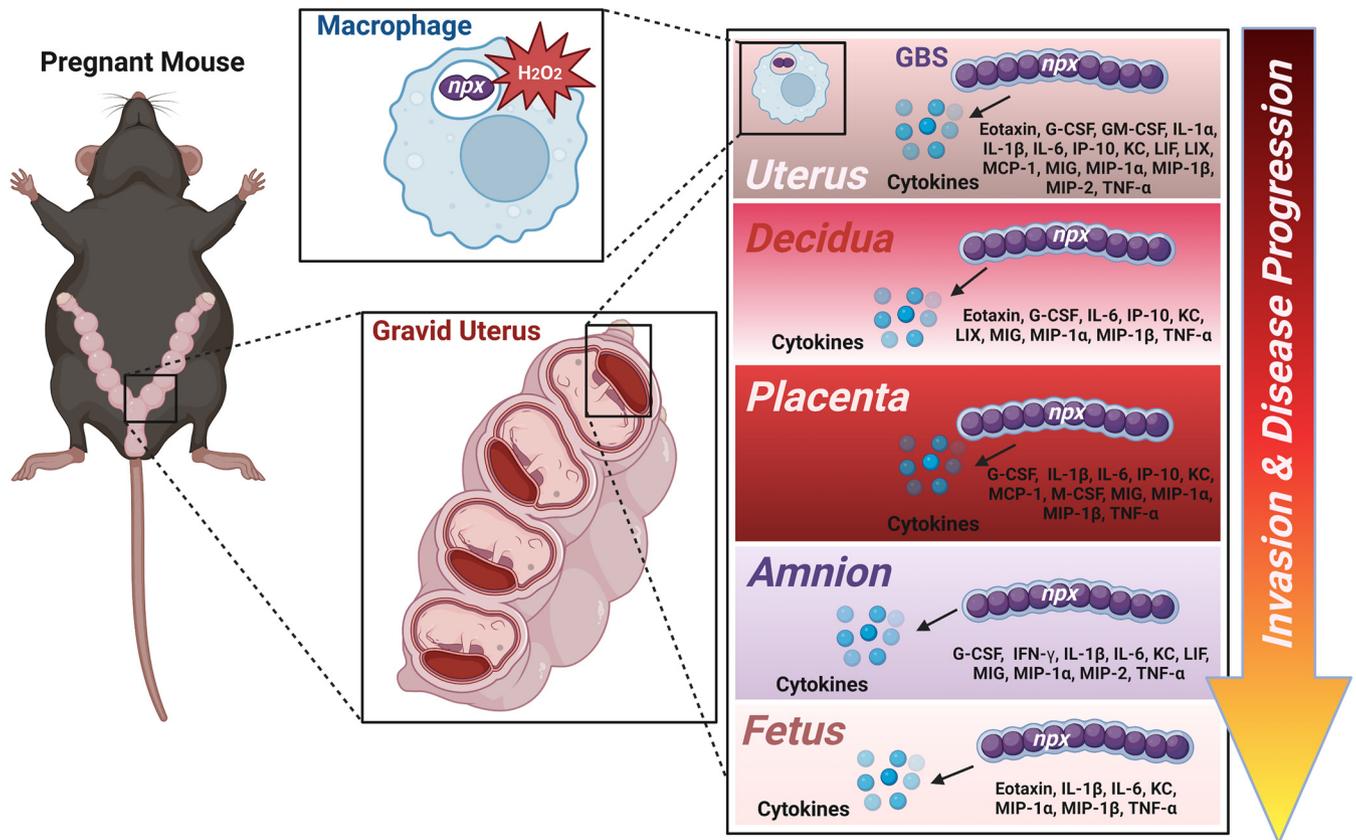
FIG 10 Conceptual model of *npx*-dependent invasion and proinflammatory signal initiation in ascending GBS infections during pregnancy. GBS ascends the reproductive tract by surviving within placental macrophages, in part by encoding an NADH peroxidase to aid in detoxifying oxidative stress (such as peroxides [H_2O_2]). GBS invasion and full burdens within the gravid reproductive tract (uterus, decidua, placenta, amnion, and fetus) require *npx* expression and trigger the production of tissue compartment-specific proinflammatory cytokines, resulting in inflammation and disease progression, including rupture of membranes, preterm birth, and maternal demise. (Image created with BioRender.com.)

gestational tissues, cognate inflammatory responses, and disease compared to the parental strain or the complemented mutant, demonstrating the importance of *npx* for pathogenesis (Fig. 10). We observed drastic reductions in the bacterial burdens in the uterus, decidua, placenta, amnion, and fetal tissue compartments derived from animals infected with the Δ*npx* mutant compared to the burdens in animals infected with the parental strain or the complemented isogenic derivative. These reductions in burdens correlated with the decreased production of proinflammatory cytokines such as IL-1β, MIP-1α, and TNF-α in all of the examined tissue compartments of the gravid reproductive tract. Interestingly, the diminutions of proinflammatory cytokine production and bacterial burdens were associated with cognate decreases in adverse pregnancy outcomes such as PPROM, preterm birth, and maternal demise. Previous work has linked high levels of IL-1β, MIP-1α, and TNF-α with an enhanced risk of preterm birth (70). It is likely that the expression of proinflammatory cytokines perturbs maternal tolerance of the semialloge-neic fetus, leading to an enhanced risk of adverse pregnancy outcomes (71). Recently, interest has been piqued in exploiting the NLRP3 inflammasome pathway as a potential chemotherapeutic strategy to ameliorate the risk associated with perinatal disease outcomes (72). Because the expression of the *npx* locus is critical for GBS ascension of the reproductive tract and the initiation of these signaling pathways that promote inflammation, a dually targeted approach of the inhibition of the GBS NADH peroxidase and the NLRP3 inflammasome pathway could prove useful in combating GBS perinatal infections.

Intracellular infection of PMs resulted in the production of proinflammatory cytokines such as G-CSF, GM-CSF, growth-regulated protein alpha (GRO-α), IL-1RA, IL-1α, IL-1β, IL-6, IL-8, MCP-1, MIP-1α, MIP-1β, and TNF-α. However, *npx* was dispensable for

this induction. This was a surprising result considering the significant differences in bacterial loads within these macrophages, underscoring that even low levels of GBS intracellular infection are sufficient to induce the production of these cytokines. The production of proinflammatory cytokines by macrophages instigates the recruitment of neutrophils in mice upon GBS infection (15, 73). A similar response has also been observed in humans (73). Neutrophils aid in the clearance of bacteria by phagocytosis and subsequent killing in internal vacuoles called phagosomes (74). Finally, neutrophils excrete neutrophil extracellular traps (NETs) loaded with various antimicrobial peptides (75). These extracellular DNA traps have been exhibited in response to GBS infection (15). Collectively, placental macrophages and neutrophils predominate the innate immune response against GBS infection.

Our studies indicate that NADH peroxidase plays an important role in the full virulence of GBS in a mouse model of ascending vaginal infection during pregnancy. Other reactive oxygen species-detoxifying enzymes such as catalase and superoxide dismutase are also important for the virulence of many bacterial pathogens, especially those that survive and establish replicative niches within macrophages (76, 77). The introduction of bacterium-specific inhibitors of oxidative stress response pathways may target bacteria without impacting the host, providing exciting new avenues for drug development. As such, developing small molecules or other chemotherapeutic strategies to inhibit these enzymes may be a viable option to defend against these bacterial infections. The identification of these bacterium-specific inhibitors is being researched currently and includes small molecules that inhibit *M. tuberculosis* catalase (78). A plausible future direction of our work may include screening preexisting banks of small molecules against purified GBS NADH peroxidase protein or creating a crystal structure to identify regions for targeted drug design.

MATERIALS AND METHODS

Bacterial strains and culture conditions. *S. agalactiae* strain GB00112 (GB112), which represents the wild-type (WT) or parental strain, was utilized in this study. GB112 is a clinical, sequence type 12 (ST-12), capsular polysaccharide (CPS) serotype III strain isolated from a rectovaginal swab of a postpartum patient (79). We previously examined GB112 for interactions with host macrophages and fetal membranes (36, 80). Isogenic GB112 mutants were constructed previously. These mutants include an *npx* deletion mutant (Δnpx) and a complemented Δnpx mutant harboring a plasmid containing the *npx* locus ($\Delta npx::c$), as previously described (36). Bacterial strains were grown on tryptic soy agar plates supplemented with 5% sheep blood or in Todd-Hewitt broth (THB) at 37°C. Derivatives harboring the pLZ12 plasmid were grown in medium supplemented with 3 μg/mL chloramphenicol. *E. coli* DH5α strains used for the mutation and complementation processes were grown in LB broth or agar supplemented with either 150 μg/mL erythromycin or 20 μg/mL chloramphenicol when necessary.

Purification of placental macrophages. Deidentified placental tissue was collected from nonlaboring women who delivered healthy, full-term infants by Caesarian section at the Vanderbilt University Medical Center with approval from the Vanderbilt University Medical Center Institutional Review Board (VUMC IRB) (approval number 181998). Placental macrophages (PMs) were isolated according to our previously described methods (80, 81). Briefly, villous core tissue was macerated and enzymatically digested with hyaluronidase, collagenase, and DNase (Sigma-Aldrich) before being strained through a stainless steel filter and suspended in RPMI 1640 with HEPES, L-glutamine, and fetal bovine serum supplemented with antibiotic and antifungal factors. Cells were filtered and centrifuged, and CD14$^+$ cells were isolated using the magnetic activated cell sorting (MACS) cell separation system with CD14 microbeads (Miltenyi Biotec). Cells were incubated in RPMI 1640 medium (Thermo Fisher) with 10% charcoal-stripped fetal bovine serum (FBS) (Thermo Fisher) and a 1% antibiotic-antimycotic solution (Thermo Fisher) overnight at 37°C in 5% carbon dioxide. The following day, PMs were suspended in RPMI 1640 medium without antibiotic-antimycotic and distributed into polystyrene plates. Cells were seeded at a density of 200,000 cells per well in a polystyrene, 24-well culture plate in RPMI 1640 with a 1% antibiotic-antimycotic solution and 10% charcoal dextran FBS (RPMI$^{+/+}$) and then incubated for 24 h in a humidified atmosphere at 37°C with 5% CO$_2$.

Coculture of GBS with placental macrophages and survival assays. PMs were cultured in RPMI 1640 medium (Thermo Fisher) with 10% charcoal-stripped fetal bovine serum (Thermo Fisher) and a 1% antibiotic-antimycotic solution (Thermo Fisher) overnight at 37°C in room air supplemented with 5% carbon dioxide. Cocultured cells were incubated at 37°C in air supplemented with 5% carbon dioxide for 1 to 24 h with medium free of the antibiotic-antimycotic solution. Macrophages were inoculated at a multiplicity of infection (MOI) of 10:1 bacteria to host cells for 1 h. Cocultures were washed with sterile medium, resuspended in fresh medium containing 100 μg/mL of gentamicin (Sigma) to kill extracellular bacteria, and further incubated for 4 h at 37°C. Gentamicin kills extracellularly located GBS but is limited in its ability to gain access to intracellular organisms. Subsequently, the samples were extensively washed with sterile phosphate-buffered saline (PBS) and dislodged with trypsin (1× 0.05% trypsin-EDTA;

Gibco). Following the collection of the PMs, the cells were lysed by the addition of 1 mL of distilled water (dH$_2$O). Cellular cytoplasmic contents were serially diluted in PBS and plated onto blood agar plates to determine the number of viable intracellular bacteria. Samples containing only bacteria were used to estimate the efficacy of antibiotic killing as a control experiment (82).

Transmission electron microscopy analyses. Cocultures of GBS and macrophages were subjected to primary fixation with 2.5% glutaraldehyde and 2.0% paraformaldehyde in 0.05 M sodium cacodylate buffer at room temperature for 24 h. Subsequently, samples were washed three times with 0.05 M sodium cacodylate buffer and subjected to a secondary fixation step with 0.1% osmium tetroxide for 15 min. Samples were washed three times with 0.05 M sodium cacodylate buffer before being sequentially dehydrated with increasing concentrations of ethanol. After dehydration, samples were embedded in resin, polymerized, and sectioned into 70- to 90-nm sections via ultramicrotomy. Sections were lifted onto nickel or copper 100-mesh grids (Electron Microscopy Sciences) and secondarily stained with 1% phosphotungstic acid. Grids were imaged with a Philips/FEI T12 transmission electron microscope to visualize intracellular bacteria. Bacteria were enumerated in a blind manner using the ImageJ software package.

Ascending vaginal infection model. GBS infection of pregnant mice and subsequent analyses were performed as previously described (15, 37). Briefly, C57BL/6J mice were purchased from Jackson Laboratories and mated in harem breeding strategies (1 male to 3 to 4 females) overnight. Pregnancy was confirmed by the presence of a vaginal mucus plug establishing the embryonic date (embryonic day 0.5 [E0.5]) the following day. On E13.5, pregnant dams were anesthetized via the inhalation of isoflurane and vaginally infected with 5×10^2 to 10^4 CFU in 0.05 mL of THB plus 10% gelatin. Uninfected controls were also maintained. Infections were allowed to progress until term (E21.5) for disease progression studies or until E15.5 for bacterial and immunological assays. Animals were euthanized by carbon dioxide asphyxiation, and necropsy was performed to harvest reproductive tissues, including the uterus, placenta, decidua, amnion, and fetus tissues.

Quantitative culture evaluation of bacterial burdens. To determine the bacterial burden in reproductive tissues, quantitative culture methods were employed, as previously described (37). Briefly, reproductive tissues were weighed and placed into sterile THB. Tissues were homogenized, subjected to serial dilution, and plated onto blood agar to quantify bacteria (CFU per milligram) in host tissue. Plates were incubated at 37°C in air supplemented with 5% carbon dioxide overnight, and individual colonies were counted to quantify CFU.

Evaluation of bacterial growth in amniotic fluid. To determine bacterial growth in human or mouse amniotic fluid, quantitative culture methods were employed, as described above. Briefly, human amniotic fluid was pipetted off the surface of the placentas from term, nonlaboring C-section deliveries. Mouse amniotic fluid was collected after necropsy on embryonic day 15.5. All amniotic fluid samples were stored at −80°C until utilization for growth assays. Amniotic fluid samples (100 L) were placed into 96-well plates, and a 1:100 dilution of a bacterial culture grown overnight (either WT GBS, the Δ*npx* mutant, or the complemented derivative) was inoculated into the amniotic fluid. Samples were incubated overnight (16 to 24 h) at 37°C in room air supplemented with 5% CO$_2$. The following day, viable bacteria were enumerated via serial dilution and plating onto bacteriological medium (blood agar plates). Plates were incubated at 37°C in room air supplemented with 5% CO$_2$ overnight, and the following day, bacterial colonies were counted to enumerate viable bacterial cells.

Evaluation of cytokine responses to GBS infection. Mouse reproductive tissues, maternal sera, and amniotic fluid were analyzed by multiplex cytokine assays. Mouse tissues were placed into 0.5 mL of sterile PBS or THB plus 10 mg/mL penicillin, homogenized, and passed through a 0.22-μm filter. Samples were frozen at −80°C or on dry ice until analyses were performed. Samples were analyzed by Eve Technologies (Alberta, Canada) via a multiplex cytokine array, as previously described (83). Validation of host targets for specific cytokines (IL-1β, IL-6, KC, and TNF-α) was performed by a sandwich enzyme-linked immunosorbent assay (ELISA) (Abcam), as indicated in our previous study (84).

Ethics statement. This study was carried out in accordance with the recommendations of the Vanderbilt University Medical Center Institutional Review Board. This protocol was approved by the IRB (approval numbers 181998 and 00005756). All animal experiments were performed in accordance with the Animal Welfare Act, U.S. federal law, and NIH guidelines. All experiments were carried out under a protocol approved by the Vanderbilt University Institutional Animal Care and Use Committee (IACUC) (approvals M/14/034, M/17/002, and V2000089), a body that has been accredited by the Association for Assessment and Accreditation of Laboratory Animal Care (AAALAC).

Statistical analyses. Statistical analysis of parametric data with more than two groups was performed using one-way ANOVA with either Tukey's or Dunnett's *post hoc* correction for multiple comparisons; all reported *P* values were adjusted to account for multiple comparisons. For parametric data with two groups, Student's *t* test or one-way ANOVA was used. *P* values of ≤0.05 were considered significant. Nonparametric data (such as log-transformed CFU data) were analyzed by Mann-Whitney U or Kruskal-Wallis tests. Disease outcome data, including survival curves, were analyzed using the Mantel-Cox log rank test and the Gehan-Breslow-Wilcoxon test. All data analyzed in this work were derived from at least three biological replicates (representing different human or mouse samples). Statistical analyses were performed using GraphPad Prism 9 (GraphPad Software Inc.).

Data availability. Data are available upon reasonable request to the authors.

SUPPLEMENTAL MATERIAL

Supplemental material is available online only.

FIG S1, TIF file, 0.4 MB.

FIG S2, TIF file, 0.8 MB.

FIG S3, TIF file, 0.9 MB.
FIG S4, TIF file, 0.7 MB.
FIG S5, TIF file, 0.7 MB.
FIG S6, TIF file, 0.6 MB.

REFERENCES

1. Goldenberg RL, Culhane JF, Iams JD, Romero R. 2008. Epidemiology and causes of preterm birth. Lancet 371:75–84. https://doi.org/10.1016/S0140-6736(08)60074-4.
2. Martin JA, Hamilton BE, Sutton PD, Ventura SJ, Menacker F, Kirmeyer S, Munson ML, Centers for Disease Control and Prevention National Center for Health Statistics National Vital Statistics System. 2007. Births: final data for 2005. Natl Vital Stat Rep 56:1–103.
3. Purisch SE, Gyamfi-Bannerman C. 2017. Epidemiology of preterm birth. Semin Perinatol 41:387–391. https://doi.org/10.1053/j.semperi.2017.07.009.
4. McCormick MC. 1985. The contribution of low birth weight to infant mortality and childhood morbidity. N Engl J Med 312:82–90. https://doi.org/10.1056/NEJM198501103120204.
5. Saigal S, Doyle LW. 2008. An overview of mortality and sequelae of preterm birth from infancy to adulthood. Lancet 371:261–269. https://doi.org/10.1016/S0140-6736(08)60136-1.
6. Goldenberg RL, Hauth JC, Andrews WW. 2000. Intrauterine infection and preterm delivery. N Engl J Med 342:1500–1507. https://doi.org/10.1056/NEJM200005183422007.
7. Doran KS, Nizet V. 2004. Molecular pathogenesis of neonatal group B streptococcal infection: no longer in its infancy. Mol Microbiol 54:23–31. https://doi.org/10.1111/j.1365-2958.2004.04266.x.
8. Patras KA, Nizet V. 2018. Group B streptococcal maternal colonization and neonatal disease: molecular mechanisms and preventative approaches. Front Pediatr 6:27. https://doi.org/10.3389/fped.2018.00027.
9. Shabayek S, Spellerberg B. 2018. Group B streptococcal colonization, molecular characteristics, and epidemiology. Front Microbiol 9:437. https://doi.org/10.3389/fmicb.2018.00437.
10. Deutscher M, Lewis M, Zell ER, Taylor TH, Jr, Van Beneden C, Schrag S, Active Bacterial Core Surveillance Team. 2011. Incidence and severity of invasive *Streptococcus pneumoniae*, group A *Streptococcus*, and group B *Streptococcus* infections among pregnant and postpartum women. Clin Infect Dis 53:114–123. https://doi.org/10.1093/cid/cir325.
11. Rao GG, Khanna P. 2020. To screen or not to screen women for group B *Streptococcus* (*Streptococcus agalactiae*) to prevent early onset sepsis in newborns: recent advances in the unresolved debate. Ther Adv Infect Dis 7:2049936120942424. https://doi.org/10.1177/2049936120942424.
12. Nanduri SA, Petit S, Smelser C, Apostol M, Alden NB, Harrison LH, Lynfield R, Vagnone PS, Burzlaff K, Spina NL, Dufort EM, Schaffner W, Thomas AR, Farley MM, Jain JH, Pondo T, McGee L, Beall BW, Schrag SJ. 2019. Epidemiology of invasive early-onset and late-onset group B streptococcal disease in the United States, 2006 to 2015: multistate laboratory and population-based surveillance. JAMA Pediatr 173:224–233. https://doi.org/10.1001/jamapediatrics.2018.4826.
13. Verani JR, McGee L, Schrag SJ, Division of Bacterial Diseases, National Center for Immunization and Respiratory Diseases, Centers for Disease Control and Prevention (CDC). 2010. Prevention of perinatal group B streptococcal disease—revised guidelines from CDC, 2010. MMWR Recommend Rep 59(RR-10):1–36.
14. Ho YR, Li CM, Yu CH, Lin YJ, Wu CM, Harn IC, Tang MJ, Chen YT, Shen FC, Lu CY, Tsai TC, Wu JJ. 2013. The enhancement of biofilm formation in group B streptococcal isolates at vaginal pH. Med Microbiol Immunol 202:105–115. https://doi.org/10.1007/s00430-012-0255-0.
15. Kothary V, Doster RS, Rogers LM, Kirk LA, Boyd KL, Romano-Keeler J, Haley KP, Manning SD, Aronoff DM, Gaddy JA. 2017. Group B *Streptococcus* induces neutrophil recruitment to gestational tissues and elaboration of extracellular traps and nutritional immunity. Front Cell Infect Microbiol 7:19. https://doi.org/10.3389/fcimb.2017.00019.
16. Kim CJ, Romero R, Chaemsaithong P, Chaiyasit N, Yoon BH, Kim YM. 2015. Acute chorioamnionitis and funisitis: definition, pathologic features, and clinical significance. Am J Obstet Gynecol 213:S29–S52. https://doi.org/10.1016/j.ajog.2015.08.040.

17. Kollmann TR, Kampmann B, Mazmanian SK, Marchant A, Levy O. 2017. Protecting the newborn and young infant from infectious diseases: lessons from immune ontogeny. Immunity 46:350–363. https://doi.org/10.1016/j.immuni.2017.03.009.

18. Yockey LJ, Iwasaki A. 2018. Interferons and proinflammatory cytokines in pregnancy and fetal development. Immunity 49:397–412. https://doi.org/10.1016/j.immuni.2018.07.017.

19. Romero R, Espinoza J, Gonçalves LF, Kusanovic JP, Friel L, Hassan S. 2007. The role of inflammation and infection in preterm birth. Semin Reprod Med 25:21–39. https://doi.org/10.1055/s-2006-956773.

20. Gibbs RS, Romero R, Hillier SL, Eschenbach DA, Sweet RL. 1992. A review of premature birth and subclinical infection. Am J Obstet Gynecol 166:1515–1528. https://doi.org/10.1016/0002-9378(92)91628-n.

21. Holst RM, Hagberg H, Wennerholm UB, Skogstrand K, Thorsen P, Jacobsson B. 2009. Prediction of spontaneous preterm delivery in women with preterm labor: analysis of multiple proteins in amniotic and cervical fluids. Obstet Gynecol 114:268–277. https://doi.org/10.1097/AOG.0b013e3181ae6a08.

22. Agrawal V, Hirsch E. 2012. Intrauterine infection and preterm labor. Semin Fetal Neonatal Med 17:12–19. https://doi.org/10.1016/j.siny.2011.09.001.

23. Triggs T, Kumar S, Mitchell M. 2020. Experimental drugs for the inhibition of preterm labor. Expert Opin Investig Drugs 29:507–523. https://doi.org/10.1080/13543784.2020.1752661.

24. Liu S, Diao L, Huang C, Li Y, Zeng Y, Kwak-Kim JYH. 2017. The role of decidual immune cells on human pregnancy. J Reprod Immunol 124:44–53. https://doi.org/10.1016/j.jri.2017.10.045.

25. Nagamatsu T, Schust DJ. 2010. The contribution of macrophages to normal and pathological pregnancies. Am J Reprod Immunol 63:460–471. https://doi.org/10.1111/j.1600-0897.2010.00813.x.

26. Thomas JR, Naidu P, Appios A, McGovern N. 2021. The ontogeny and function of placental macrophages. Front Immunol 12:771054. https://doi.org/10.3389/fimmu.2021.771054.

27. Brown MB, von Chamier M, Allam AB, Reyes L. 2014. M1/M2 macrophage polarity in normal and complicated pregnancy. Front Immunol 5:606. https://doi.org/10.3389/fimmu.2014.00606.

28. Reyes L, Wolfe B, Golos T. 2017. Hofbauer cells: placental macrophages of fetal origin. Results Probl Cell Differ 62:45–60. https://doi.org/10.1007/978-3-319-54090-0_3.

29. Doster RS, Sutton JA, Rogers LM, Aronoff DM, Gaddy JA. 2018. *Streptococcus agalactiae* induces placental macrophages to release extracellular traps loaded with tissue remodeling enzymes via an oxidative burst-dependent mechanism. mBio 9:e02084-18. https://doi.org/10.1128/mBio.02084-18.

30. Ezraty B, Gennaris A, Barras F, Collet JF. 2017. Oxidative stress, protein damage and repair in bacteria. Nat Rev Microbiol 15:385–396. https://doi.org/10.1038/nrmicro.2017.26.

31. Lemire J, Alhasawi A, Appanna VP, Tharmalingam S, Appanna VD. 2017. Metabolic defence against oxidative stress: the road less travelled so far. J Appl Microbiol 123:798–809. https://doi.org/10.1111/jam.13509.

32. Slauch JM. 2011. How does the oxidative burst of macrophages kill bacteria? Still an open question. Mol Microbiol 80:580–583. https://doi.org/10.1111/j.1365-2958.2011.07612.x.

33. Poyart C, Pellegrini E, Gaillot O, Boumaila C, Baptista M, Trieu-Cuot P. 2001. Contribution of Mn-cofactored superoxide dismutase (SodA) to the virulence of *Streptococcus agalactiae*. Infect Immun 69:5098–5106. https://doi.org/10.1128/IAI.69.8.5098-5106.2001.

34. Janowiak BE, Griffith OW. 2005. Glutathione synthesis in *Streptococcus agalactiae*. One protein accounts for gamma-glutamylcysteine synthetase and glutathione synthetase activities. J Biol Chem 280:11829–11839. https://doi.org/10.1074/jbc.M414326200.

35. Liu GY, Doran KS, Lawrence T, Turkson N, Puliti M, Tissi L, Nizet V. 2004. Sword and shield: linked group B streptococcal β-hemolysin/cytolysin and carotenoid pigment function to subvert host phagocyte defense. Proc Natl Acad Sci U S A 101:14491–14496. https://doi.org/10.1073/pnas.0406143101.

36. Korir ML, Flaherty RA, Rogers LM, Gaddy JA, Aronoff DM, Manning SD. 2018. Investigation of the role that NADH peroxidase plays in oxidative stress survival in group B *Streptococcus*. Front Microbiol 9:2786. https://doi.org/10.3389/fmicb.2018.02786.

37. Noble K, Lu J, Guevara MA, Doster RS, Chambers SA, Rogers LM, Moore RE, Spicer SK, Eastman AJ, Francis JD, Manning SD, Rajagopal L, Aronoff DM, Townsend SD, Gaddy JA. 2021. Group B *Streptococcus cpsE* is required for serotype V capsule production and aids in biofilm formation and ascending infection of the reproductive tract during pregnancy. ACS Infect Dis 7:2686–2696. https://doi.org/10.1021/acsinfecdis.1c00182.

38. Korir ML, Doster RS, Lu J, Guevara MA, Spicer SK, Moore RE, Francis JD, Rogers LM, Haley KP, Blackman A, Noble KN, Eastman AJ, Williams JA, Damo SM, Boyd KL, Townsend SD, Henrique Serezani C, Aronoff DM, Manning SD, Gaddy JA. 2022. *Streptococcus agalactiae cadD* alleviates metal stress and promotes intracellular survival in macrophages and ascending infection during pregnancy. Nat Commun 13:5392. https://doi.org/10.1038/s41467-022-32916-7.

39. Houser BL, Tilburgs T, Hill J, Nicotra ML, Strominger JL. 2011. Two unique human decidual macrophage populations. J Immunol 186:2633–2642. https://doi.org/10.4049/jimmunol.1003153.

40. Sutton JA, Rogers LM, Dixon BREA, Kirk L, Doster R, Algood HM, Gaddy JA, Flaherty R, Manning SD, Aronoff DM. 2019. Protein kinase D mediates inflammatory responses of human placental macrophages to group B *Streptococcus*. Am J Reprod Immunol 81:e13075. https://doi.org/10.1111/aji.13075.

41. Garai P, Berry L, Moussouni M, Bleves S, Blanc-Potard AB. 2019. Killing from the inside: intracellular role of T3SS in the fate of *Pseudomonas aeruginosa* within macrophages revealed by *mgtC* and *oprF* mutants. PLoS Pathog 15:e1007812. https://doi.org/10.1371/journal.ppat.1007812.

42. Connor MG, Pulsifer AR, Price CT, Abu Kwaik Y, Lawrenz MB. 2015. *Yersinia pestis* requires host Rab1b for survival in macrophages. PLoS Pathog 11:e1005241. https://doi.org/10.1371/journal.ppat.1005241.

43. Kang YS, Kirby JE. 2019. A chemical genetics screen reveals influence of p38 mitogen-activated protein kinase and autophagy on phagosome development and intracellular replication of *Brucella neotomae* in macrophages. Infect Immun 87:e00044-19. https://doi.org/10.1128/IAI.00044-19.

44. Demarre G, Prudent V, Schenk H, Rousseau E, Bringer M-A, Barnich N, Tran Van Nhieu G, Rimsky S, De Monte S, Espéli O. 2019. The Crohn's disease-associated *Escherichia coli* strain LF82 relies on SOS and stringent responses to survive, multiply and tolerate antibiotics within macrophages. PLoS Pathog 15:e1008123. https://doi.org/10.1371/journal.ppat.1008123.

45. Château A, Seifert HS. 2016. *Neisseria gonorrhoeae* survives within and modulates apoptosis and inflammatory cytokine production of human macrophages. Cell Microbiol 18:546–560. https://doi.org/10.1111/cmi.12529.

46. Isberg RR, O'Connor TJ, Heidtman M. 2009. The *Legionella pneumophila* replication vacuole: making a cosy niche inside host cells. Nat Rev Microbiol 7:13–24. https://doi.org/10.1038/nrmicro1967.

47. Ercoli G, Fernandes VE, Chung WY, Wanford JJ, Thomson S, Bayliss CD, Straatman K, Crocker PR, Dennison A, Martinez-Pomares L, Andrew PW, Moxon ER, Oggioni MR. 2018. Intracellular replication of *Streptococcus pneumoniae* inside splenic macrophages serves as a reservoir for septicaemia. Nat Microbiol 3:600–610. https://doi.org/10.1038/s41564-018-0147-1.

48. O'Neill AM, Thurston TLM, Holden DW. 2016. Cytosolic replication of group A *Streptococcus* in human macrophages. mBio 7:e00931-16. https://doi.org/10.1128/mBio.00931-16.

49. Scherer AK, Blair BA, Park J, Seman BG, Kelley JB, Wheeler RT. 2020. Redundant Trojan horse and endothelial-circulatory mechanisms for host-mediated spread of *Candida albicans* yeast. PLoS Pathog 16:e1008414. https://doi.org/10.1371/journal.ppat.1008414.

50. Goenka A, Casulli J, Hussell T. 2018. *Mycobacterium tuberculosis* joyrides alveolar macrophages into the pulmonary interstitium. Cell Host Microbe 24:331–333. https://doi.org/10.1016/j.chom.2018.08.011.

51. Njiri OA, Zhang X, Zhang Y, Wu B, Jiang L, Li Q, Liu W, Chen T. 2020. CD209 C-type lectins promote host invasion, dissemination, and infection of *Toxoplasma gondii*. Front Immunol 11:656. https://doi.org/10.3389/fimmu.2020.00656.

52. Horn J, Stelzner K, Rudel T, Fraunholz M. 2018. Inside job: *Staphylococcus aureus* host-pathogen interactions. Int J Med Microbiol 308:607–624. https://doi.org/10.1016/j.ijmm.2017.11.009.

53. Davis MJ, Eastman AJ, Qiu Y, Gregorka B, Kozel TR, Osterholzer JJ, Curtis JL, Swanson JA, Olszewski MA. 2015. *Cryptococcus neoformans*-induced macrophage lysosome damage crucially contributes to fungal virulence. J Immunol 194:2219–2231. https://doi.org/10.4049/jimmunol.1402376.

54. Zuck M, Ellis T, Venida A, Hybiske K. 2017. Extrusions are phagocytosed and promote *Chlamydia* survival within macrophages. Cell Microbiol 19:e12683. https://doi.org/10.1111/cmi.12683.

55. Bryan ER, Kollipara A, Trim LK, Armitage CW, Carey AJ, Mihalas B, Redgrove KA, McLaughlin EA, Beagley KW. 2019. Hematogenous dissemination of *Chlamydia muridarum* from the urethra in macrophages causes testicular infection and sperm DNA damage. Biol Reprod 101:748–759. https://doi.org/10.1093/biolre/ioz146.

56. Leseigneur C, Lê-Bury P, Pizarro-Cerdá J, Dussurget O. 2020. Emerging evasion mechanisms of macrophage defenses by pathogenic bacteria.

Front Cell Infect Microbiol 10:577559. https://doi.org/10.3389/fcimb.2020.577559.

57. Malathi M, Sowmya V, Vijayalakshmi A, Prasad P, Singh N, Das B, Raisuddin S, Dudeja M, Rastogi S. 2016. Differential expression of superoxide dismutases in early aborters infected with *Chlamydia trachomatis*. Int J Infect Dis 45:203–204. https://doi.org/10.1016/j.ijid.2016.02.467.

58. Seib KL, Wu H-J, Kidd SP, Apicella MA, Jennings MP, McEwan AG. 2006. Defenses against oxidative stress in *Neisseria gonorrhoeae*: a system tailored for a challenging environment. Microbiol Mol Biol Rev 70:344–361. https://doi.org/10.1128/MMBR.00044-05.

59. Sharma RK, Agarwal A. 2004. Role of reactive oxygen species in gynecologic diseases. Reprod Med Biol 3:177–199. https://doi.org/10.1111/j.1447-0578.2004.00068.x.

60. Park B, Nizet V, Liu GY. 2008. Role of *Staphylococcus aureus* catalase in niche competition against *Streptococcus pneumoniae*. J Bacteriol 190:2275–2278. https://doi.org/10.1128/JB.00006-08.

61. Elkins JG, Hassett DJ, Stewart PS, Schweizer HP, McDermott TR. 1999. Protective role of catalase in *Pseudomonas aeruginosa* biofilm resistance to hydrogen peroxide. Appl Environ Microbiol 65:4594–4600. https://doi.org/10.1128/AEM.65.10.4594-4600.1999.

62. Su S, Panmanee W, Wilson JJ, Mahtani HK, Li Q, VanderWielen BD, Makris TM, Rogers M, McDaniel C, Lipscomb JD, Irvin RT, Schurr MJ, Lancaster JR, Kovall RA, Hassett DJ. 2014. Catalase (KatA) plays a role in protection against anaerobic nitric oxide in *Pseudomonas aeruginosa*. PLoS One 9: e91813. https://doi.org/10.1371/journal.pone.0091813.

63. Hochman A, Goldberg I. 1991. Purification and characterization of a catalase-peroxidase and a typical catalase from the bacterium *Klebsiella pneumoniae*. Biochim Biophys Acta 1077:299–307. https://doi.org/10.1016/0167-4838(91)90544-A.

64. Manca C, Paul S, Barry CE, III, Freedman VH, Kaplan G. 1999. *Mycobacterium tuberculosis* catalase and peroxidase activities and resistance to oxidative killing in human monocytes in vitro. Infect Immun 67:74–79. https://doi.org/10.1128/IAI.67.1.74-79.1999.

65. Gregory EM, Yost FJ, Fridovich I. 1973. Superoxide dismutases of *Escherichia coli*: intracellular localization and functions. J Bacteriol 115:987–991. https://doi.org/10.1128/jb.115.3.987-991.1973.

66. de Groote MA, Ochsner UA, Shiloh MU, Nathan C, McCord JM, Dinauer MC, Libby SJ, Vazquez-Torres A, Xu Y, Fang FC. 1997. Periplasmic superoxide dismutase protects *Salmonella* from products of phagocyte NADPH-oxidase and nitric oxide synthase. Proc Natl Acad Sci U S A 94:13997–14001. https://doi.org/10.1073/pnas.94.25.13997.

67. Vanaporn M, Wand M, Michell SL, Sarkar-Tyson M, Ireland P, Goldman S, Kewcharoenwong C, Rinchai D, Lertmemongkolchai G, Titball RW. 2011. Superoxide dismutase C is required for intracellular survival and virulence of *Burkholderia pseudomallei*. Microbiology (Reading) 157:2392–2400. https://doi.org/10.1099/mic.0.050823-0.

68. Lien KA, Dinshaw K, Nichols RJ, Cassidy-Amstutz C, Knight M, Singh R, Eltis LD, Savage DF, Stanley SA. 2021. A nanocompartment system contributes to defense against oxidative stress in *Mycobacterium tuberculosis*. Elife 10:e74358. https://doi.org/10.7554/eLife.74358.

69. Cesinger MR, Schwardt NH, Halsey CR, Thomason MK, Reniere ML. 2021. Investigating the roles of *Listeria monocytogenes* peroxidases in growth and virulence. Microbiol Spectr 9:e00440-21. https://doi.org/10.1128/Spectrum.00440-21.

70. Rodríguez-Benítez MV, Gámez-Belmonte R, Gil-Campos M, Hernández-Chirlaque C, Bouzas PR, Sánchez de Medina F, Martínez-Augustin O. 2021. Premature birth infants present elevated inflammatory markers in the meconium. Front Pediatr 8:627475. https://doi.org/10.3389/fped.2020.627475.

71. Ding J, Zhang Y, Cai X, Diao L, Yang C, Yang J. 2021. Crosstalk between trophoblast and macrophage at the maternal-fetal interface: current status and future perspectives. Front Immunol 12:758281. https://doi.org/10.3389/fimmu.2021.758281.

72. Zhou F, Li C, Zhang SY. 2020. NLRP3 inflammasome: a new therapeutic target for high-risk reproductive disorders? Chin Med J (Engl) 134:20–27. https://doi.org/10.1097/CM9.0000000000001214.

73. Carey AJ, Tan CK, Mirza S, Irving-Rodgers H, Webb RI, Lam A, Ulett GC. 2014. Infection and cellular defense dynamics in a novel 17β-estradiol murine model of chronic human group B streptococcus genital tract colonization reveal a role for hemolysin in persistence and neutrophil accumulation. J Immunol 192:1718–1731. https://doi.org/10.4049/jimmunol.1202811.

74. Winterbourn CC, Kettle AJ, Hampton MB. 2016. Reactive oxygen species and neutrophil function. Annu Rev Biochem 85:765–792. https://doi.org/10.1146/annurev-biochem-060815-014442.

75. Brinkmann V, Laube B, Abed UA, Goosmann C, Zychlinsky A. 2010. Neutrophil extracellular traps: how to generate and visualize them. J Vis Exp 2010:1724. https://doi.org/10.3791/1724.

76. Yuan F, Yin S, Xu Y, Xiang L, Wang H, Li Z, Fan K, Pan G. 2021. The richness and diversity of catalases in bacteria. Front Microbiol 12:645477. https://doi.org/10.3389/fmicb.2021.645477.

77. Broxton CN, Culotta VC. 2016. SOD enzymes and microbial pathogens: surviving the oxidative storm of infection. PLoS Pathog 12:e1005295. https://doi.org/10.1371/journal.ppat.1005295.

78. Jangam CS, Bhowmick S, Chorge RD, Bharatrao LD, Patil PC, Chikhale RV, AlFaris NA, ALTamimi JZ, Wabaidur SM, Islam MA. 2019. Pharmacoinformatics-based identification of anti-bacterial catalase-peroxidase enzyme inhibitors. Comput Biol Chem 83:107136. https://doi.org/10.1016/j.compbiolchem.2019.107136.

79. Manning SD, Lewis MA, Springman AC, Lehotzky E, Whittam TS, Davies HD. 2008. Genotypic diversity and serotype distribution of group B *Streptococcus* isolated from women before and after delivery. Clin Infect Dis 46:1829–1837. https://doi.org/10.1086/588296.

80. Lu J, Francis JD, Guevara MA, Moore RE, Chambers SA, Doster RS, Eastman AJ, Rogers LM, Noble KN, Manning SD, Damo SM, Aronoff DM, Townsend SD, Gaddy JA. 2021. Antibacterial and anti-biofilm activity of the human breast milk glycoprotein lactoferrin against group B *Streptococcus*. Chembiochem 22:2124–2133. https://doi.org/10.1002/cbic.202100016.

81. Tetz LM, Aronoff DM, Loch-Caruso R. 2015. Mono-ethylhexyl phthalate stimulates prostaglandin secretion in human placental macrophages and THP-1 cells. Reprod Biol Endocrinol 13:56. https://doi.org/10.1186/s12958-015-0046-8.

82. Medina E, Goldmann O, Toppel AW, Chhatwal GS. 2003. Survival of *Streptococcus pyogenes* within host phagocytic cells: a pathogenic mechanism for persistence and systemic invasion. J Infect Dis 187:597–603. https://doi.org/10.1086/373998.

83. Elling R, Robinson EK, Shapleigh B, Liapis SC, Covarrubias S, Katzman S, Groff AF, Jiang Z, Agarwal S, Motwani M, Chan J, Sharma S, Hennessy EJ, FitzGerald GA, McManus MT, Rinn JL, Fitzgerald KA, Carpenter S. 2018. Genetic models reveal cis and trans immune-regulatory activities for lincRNA-Cox2. Cell Rep 25:1511–1524.e6. https://doi.org/10.1016/j.celrep.2018.10.027.

84. Doster RS, Kirk LA, Tetz LM, Rogers LM, Aronoff DM, Gaddy JA. 2017. *Staphylococcus aureus* infection of human gestational membranes induces bacterial biofilm formation and host production of cytokines. J Infect Dis 215:653–657. https://doi.org/10.1093/infdis/jiw300.